Biomass Conv. Bioref.
DOI 10.1007/s13399-017-0248-8

ORIGINAL ARTICLE

Fundamentals of Hydrofaction™: Renewable crude oil from woody biomass

Claus Uhrenholt Jensen[1] · **Julie Katerine Rodriguez Guerrero**[2] · **Sergios Karatzos**[2] · **Göran Olofsson**[1] · **Steen Brummerstedt Iversen**[1]

Received: 10 October 2016 / Revised: 2 February 2017 / Accepted: 8 February 2017

Abstract As a response to the global requirement for renewable transportation fuels that are economically viable and fungible with existing petroleum infrastructure, Steeper Energy is commercializing its proprietary hydrothermal liquefaction (HTL) technology as a potential path to sustainable lignocellulosic-derived transport fuels. Hydrofaction™ utilizes high-density, supercritical water chemistry at distinctly higher pressures and temperatures than most literature on HTL. The paper presents a direct relation between density and the chemical properties that make near-critical water an appealing HTL reaction medium. Further, the fundamentals of Hydrofaction™ and how these are carefully chosen to favor certain chemical reaction paths are explained, including the use of high-density supercritical water, homogenous alkaline metal catalysts at alkaline conditions and recycling of aqueous and oil products. Steady state operational data from a campaign producing 1 barrel (>150 kg) of oil at a dedicated pilot plant is presented, including closure of mass, energy, and three elemental balances. A detailed oil assay specifying the oil quality as well as mass and energy recoveries from wood to oil of 45.3 wt.% and 85.6%, respectively, reflect that Hydrofaction™ is an energy-efficient technology for sourcing renewable biofuels in tangible volumes.

Keywords Hydrofaction™ · Hydrothermal liquefaction · Supercritical water · Biofuel · Renewable oil

✉ Steen Brummerstedt Iversen
si@steeperenergy.com

[1] Steeper Energy ApS, Sandbjergvej 11, 2970 Hørsholm, Denmark

[2] Steeper Energy Canada Ltd, Suite 200, 1210 11th Avenue S.W., Calgary T3C 0M4, Canada

1 Introduction

Petroleum is currently the lifeblood of technologically advanced civilization, and it is consumed at a rate of 94 million barrels a day globally [1]. The oil industry is sourcing these significant volumes of crude oil and refining them into transportation fuels and petrochemicals for solvents, polymers, and other higher-value materials. However, petroleum is finite and its consumption generates greenhouse gasses (GHGs) that raise climate change concerns. Industry is constantly extracting fossil carbon that is later combusted and becoming a net contributor of CO_2 and other GHGs into the Earth's atmosphere. Moreover, global reserves of good quality light sweet crude are diminishing and are mainly located in politically unstable areas. As such, the oil and gas industry, arguably the biggest industry in the world, is currently facing political, environmental, and economic challenges.

To counter these challenges, the world is turning towards new technologies that help reduce dependency on petroleum. Such alternatives include renewable transportation fuels. Vehicles fueled with electricity from renewable energy are one of these alternatives, but it requires new fuel distribution infrastructure and is mostly applicable to urban and short-distance transportation. Long-distance transportation sectors such as marine, heavy trucking, rail, and aviation cannot be readily electrified and thus have a unique dependency on liquid biofuels that are fungible with bunker, diesel, and jet fuels.

Ethanol and biodiesel are the two most widely available commercial biofuels, but they are highly oxygenated and are mostly blended in small percentages (except modified engines such as E85 in the USA and Sweden or E100 in Brazil) in gasoline and diesel road transport fuels. These oxygenates are not suitable for long-distance transportation such as aviation, heavy road freight, and marine, which require energy-dense biofuels that are functionally indistinguishable ("drop-in") to

Published online: 23 February 2017

the fossil equivalents. For example, in commercial airplanes, the total weight of fuel at takeoff is higher than the total weight of the payload (e.g., cargo and passengers) [2], which make high-energy density fuels indispensable.

Hydrotreated vegetable oils and animal fats (collectively known as hydrogenation-derived esters and fatty acids or HEFAs) are a recent non-oxygenated biofuel addition to the two main commercial biofuels. However, HEFAs are derived from fatty acid raw materials that are costly and can compete with food end uses [3]. Thermochemical biomass conversion technologies such as gasification, pyrolysis, and hydrothermal liquefaction (HTL) are being developed in order to produce advanced drop-in biofuel blendstock from non-food and lower-cost lignocellulosic biomass.

HTL is currently viewed with the potential to become a competitive and resource effective pathway to advanced biofuels from lignocellulosic biomass, mainly due to its high-energy efficiency. For example, a 2014 US DOE-commissioned study has determined that hydrotreated HTL biofuel is cheaper than the fast pyrolysis equivalent on both mass and energy bases. Additionally, the study estimates 70% GHG emission savings on HTL biofuel from wood compared to the 2005 petroleum baseline [4].

Hydrofaction™ utilizes a unique combination of supercritical water chemistry and homogenous catalysts to efficiently convert biomass residues directly to a high-energy density renewable crude oil. The present article presents the fundamentals of the Hydrofaction™ process and the reasoning behind each parameter. This includes the use of water at supercritical, high-density conditions; the use of homogenous alkaline metal catalysts; and recycling of aqueous and oil products back into the process. Furthermore, the major chemical reaction paths and their contribution during conversion are discussed.

While most HTL results in the public domain come from small-scale batch experiments, Hydrofaction™ has been proven in a continuous pilot facility. The second part of the article presents mass, energy, and elemental balances from operating this pilot plant as well as characterization data of the produced energy-dense and free-flowing oil.

1.1 Subcritical or supercritical HTL and the importance of density

The critical point of water, which is given in the phase diagram of Fig. 1, is often used to distinguish between liquefaction and gasification hydrothermal processes. HTL is often considered to take place mainly via ionic type of reactions near or below the critical point at temperatures of approximately 280–374 °C and at a pressure of at least the saturation pressure of water to avoid boiling. In contrast, hydrothermal gasification or supercritical water gasification is considered to occur mainly via radical type of reactions at supercritical temperatures or above, typically in the range of 450–600 °C and at pressures in the range of 50 to 250 bar [5, 6]. Contrary to most HTL processes, Hydrofaction™ is carried out above the critical point of water at 300–350 bar and 390–420 °C, in the transition between liquefaction and supercritical water gasification according to the general perception described above. However, due to the higher pressure of Hydrofaction™, key thermodynamic properties of water such as density and derived properties can be maintained at the same order of magnitude as for the subcritical conditions, while taking advantage of faster kinetics at higher temperatures.

Numerous HTL studies have been published on either the effect of operating temperature or pressure on product yields, coking propensity, oil quality, etc. [5, 6, 8, 9]. However, the chemical properties that make near-critical water an appealing reaction medium for HTL is a direct function of density and only indirectly of pressure and temperature. This is visualized in Fig. 2, where the ionic product and dielectric constant of water are given as a function of density for different isobars. A certain density can be obtained at different combinations of both subcritical and supercritical temperatures and pressures; however, the chemical kinetics and relative reaction rates may be very different at different temperatures. Thus, the different reaction regimes are better represented by density and temperature than the commonly used pressure and temperature. Finally, the transition from liquefaction to gasification regime is not instantaneous but occurs via a gradual transition, and this phenomenon is utilized in Hydrofaction™.

The rationale behind the relatively high operating pressures applied in Hydrofaction™ is thus to ensure a certain relatively

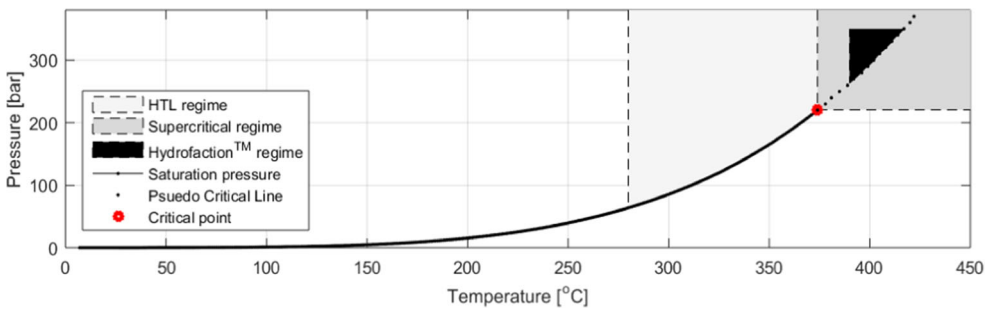

Fig. 1 Phase diagram of water to visualize the different operating regimes. Data source [7]

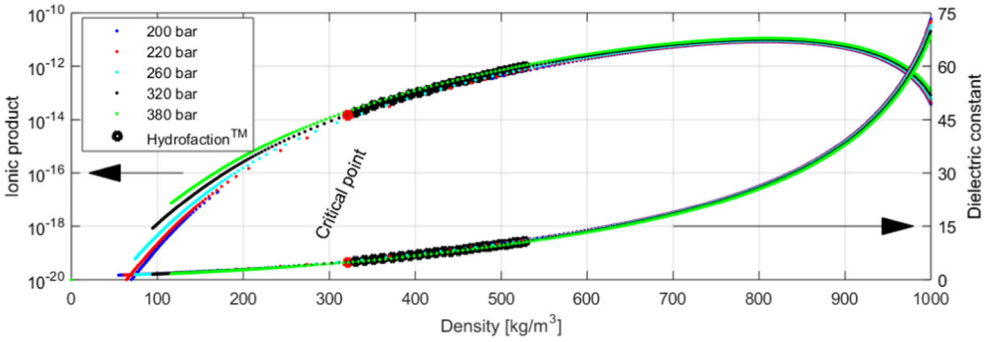

Fig. 2 Ionic product and dielectric constant of water as function of density for different isobars. Data source [7]

high density, while taking advantage of the benefits of higher temperatures. Further details on the specific choice of operating conditions are based on the changes several thermophysical properties undergo around the critical point of water.

2 Fundamentals of Hydrofaction™

The Hydrofaction™ technology platform is rooted in the generic field of hydrothermal liquefaction and is based on catalytic supercritical water chemistry. The technology applies a number of features [10]:

- Operation above the critical point of water at relatively high pressures (300–350 bar) and temperatures (390–420 °C);
- Recirculation of produced organic compounds in the form of water-soluble organics and oil for improved feed characteristics, improved energy balance, desired chemical kinetics, and improved oil yields;
- Use of homogeneous catalyst in the form of potassium carbonate (K_2CO_3) for desired catalytic effects;
- Control of pH to alkaline conditions for desired catalytic effects and minimization of corrosion;
- Recovery and recycling of homogeneous catalysts for improved process economics;
- Self-sustaining with process heat when in steady state.

The reasoning behind each of the fundamentals listed above will be specified in detail in the following.

2.1 How does Hydrofaction™ take advantage of supercritical water chemistry?

Water near its critical point obtains thermophysical properties which are very different from those at ambient conditions. The

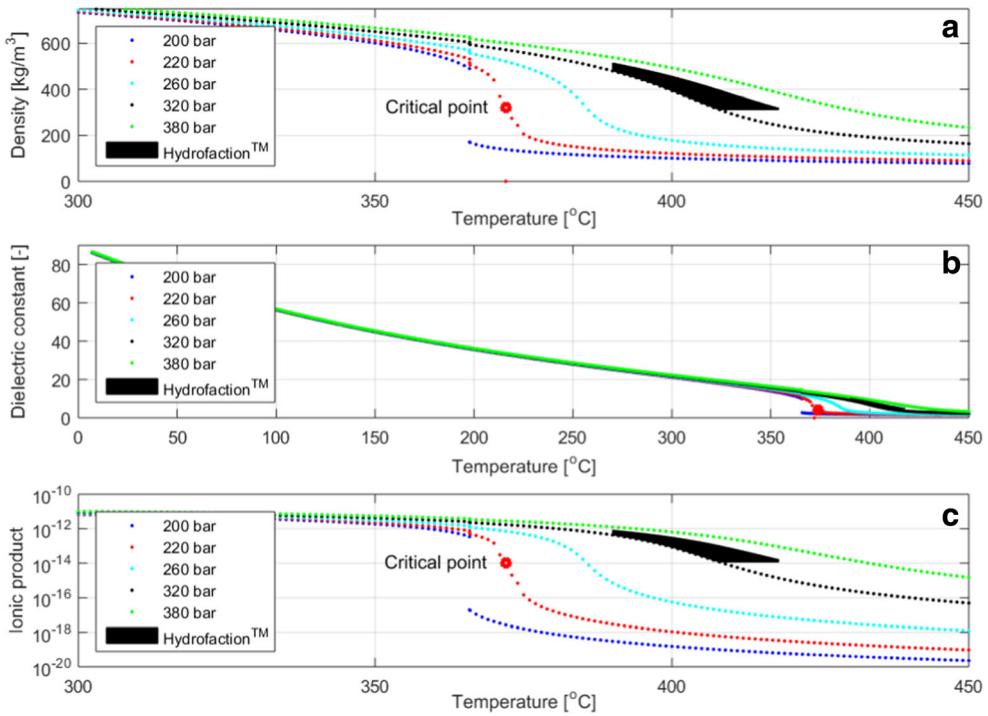

Fig. 3 Thermophysical properties of water behavior at temperatures and pressures above the critical point of water. **a** Density. **b** Dielectric constant. **c** Ionic product. Data source [7]

dielectric constant is significantly reduced making near-critical water a non-polar solvent. Additionally, the ionic product of water is very dependent on pressure around the critical temperature, and supercritical water can facilitate both ionic and radical reactions. Finally, interphase mass and heat transfer resistances are significantly reduced and mass and heat transfer rates are enhanced. The exploitation of these properties is being maximized by carefully selecting the operating conditions and configuration of the process.

Hydrofaction™ is applying a relatively high operating pressure to ensure a certain, relatively high density, while taking advantage of the benefits of supercritical temperatures. In Fig. 3a, it is clear that the relatively high-pressure range, although supercritical, sustains a high-density as compared to most HTL processes that operate near the critical point of water. Figure 3a also reveals how higher pressures reduce the gradient of density change with temperature. Considering the direct influence density has on key properties, a smoother transition is beneficial since small-temperature deviations during plant operations thereby have less impact on the important properties. For example, the 220-bar isobar in Fig. 3a reveals how density is reduced by 50% with a 5–10 °C temperature increase around the critical point. This would be undesirable from a plant operation standpoint as it would significantly alter process parameters such as retention times, fluid velocities, Reynolds numbers, and heat transfer coefficients.

The polarity of water also diminishes as water gets closer to its supercritical state as shown by the dielectric constant plotted against temperature at different pressures in Fig. 3b. The dielectric constant drops from around 85 at ambient water conditions to below 10 at and around the supercritical point of water. This allows water to dissolve biomass and biocrude molecules that are hydrophobic at ambient conditions. Such molecules include phenolics and polyaromatic hydrocarbons derived from lignin. The higher pressure applied in Hydrofaction™ slightly elevates the dielectric constant compared to the critical point. Although, it is still reduced by more than 90% as compared to ambient conditions, which facilitate solubility of non-polar compounds.

Self-ionization of water, expressed as the ionic product in Fig. 3c, is a crucial parameter within HTL because it reflects whether the reaction medium favors ionic ($>10^{-14}$) or radical ($<10^{-14}$) reactions [11, 12]. Radical reactions are in most cases undesirable due to the risk of extensive coke formation. These radical reactions are minimized below the critical point, where the ionic product is relatively high regardless of pressure. Further, the isobars are more or less identical below the critical point as seen in Fig. 3a–c, whereas a sudden drop in the ionic product is observed at lower pressures around the critical point of water. However, as shown in Fig. 3c, the high pressures of the process sustain a high ionic product despite the supercritical temperatures, thus minimizing radical reactions. In fact, the ionic product of water at Hydrofaction™ conditions can be an order of magnitude higher than for ambient water and up to several orders of magnitude higher than at the critical point.

The specific heat capacity and heat transfer properties of water change dramatically around the critical point, or more specifically around the pseudo-critical line (PCL), which influence the energy requirements of the process. The effect of operating pressure on heat requirement for an isobaric temperature increase from ambient water is visualized with specific enthalpy in Fig. 4a. At near-critical pressures, the specific enthalpy of water increases sharply around the critical point. This increase is less distinct at higher pressures, which is because the maximum specific heat capacity (PCL) is significantly reduced at higher pressures [7]. In fact, the energy required to heat water to 400 °C at 300 bar is lower than that required to heat water to the critical point at the saturation pressure. In other words, due to the elevated pressure, the additional energy required to operate at supercritical conditions compared to subcritical is insubstantial.

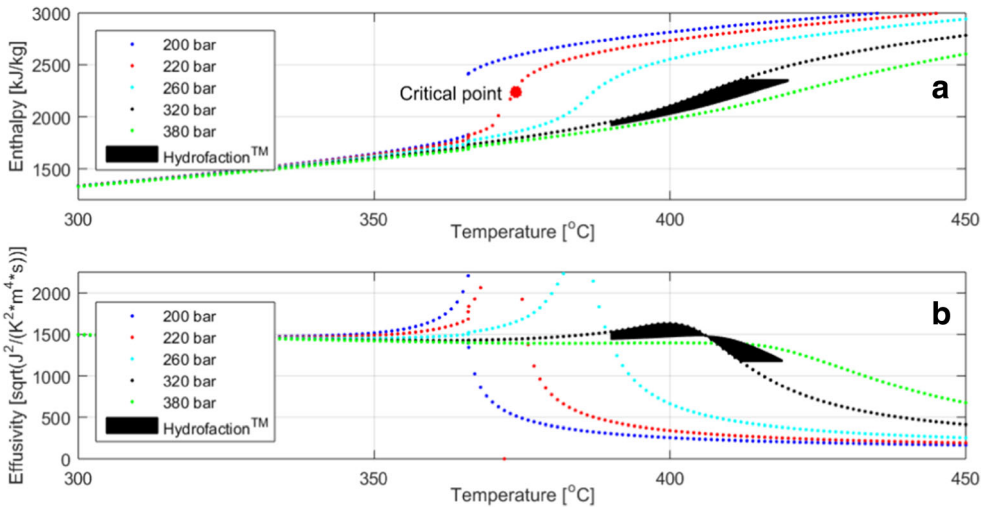

Fig. 4 Water's heat capacity and effusivity as function of temperature and pressure. **a** Enthalpy. **b** Effusivity. Data source [7]

Finally, a higher operating temperature results in a higher driving force during heat exchange, which both improves the economics of heat recovery as well as the overall energy efficiency.

The heat transfer properties of water are known to deteriorate at supercritical conditions. Figure 4b visualizes this characteristic through thermal effusivity, which reflects the ability of a substance to exchange heat with its surroundings. It is a direct function of density, specific heat capacity, and thermal conductivity. The peak at each isobar in Fig. 4b represents the PCL at which the specific heat capacity is highest. At near-critical pressures, the thermal effusivity of water sharply decreases at the critical temperature. However, at higher supercritical pressures, the thermal effusivity is sustained higher and suggests that the thermal resistance of the boundary layer is reduced at pressures above the critical [13]. At Hydrofaction™ conditions, the thermal effusivity of water is close to a maximum, exploiting a synergetic effect of the PCL, a higher density, and thermal conductivity. Theoretically, a much higher maximum can be obtained at lower pressures, but such peaks are difficult to take advantage of due to the drastic changes within a very narrow temperature range. This emphasizes how the process conditions are carefully chosen to also improve energy and heat transfer efficiency.

The above discussion is largely focused around the properties of supercritical water. Although supercritical water constitutes an important part of the process, it will typically only make up about 50 wt.% of the fluid; hence, the critical point of water is only partially relevant. The remaining 50 wt.% consists of biomass, recycled organics, Hydrofaction™ oil, and gas, depending on location in the process. The presence and recirculation of these components have several beneficial effects, which will be specified in the following sections.

2.2 Benefits of aqueous phase recirculation

The aqueous product consists of water, water-soluble organics, dissolved homogeneous catalyst, and dissolved salts from the biomass feedstock. Recirculation of this mixture reduces the makeup of the homogeneous catalyst, and the water-soluble organics are beneficial during pre-treatment and conversion. In Hydrofaction™, aqueous phase recirculation is performed by extraction and purification of the same amount of water as deducted from the feedstock biomass, while concentrating and recycling the remainder of the aqueous product. A bleed of 5–15% of the water phase is required to prevent buildup of trace components such as chloride. The bleed is further treated and purified to dischargeable or recyclable water quality.

The recycled water-soluble organics are mainly C_1–C_4 alcohols, ketones, phenols, catechols, and smaller organic acids produced by the process. They are beneficial for the pre-treatment to produce a pumpable slurry, as a dissolution mechanism is introduced in parallel with the hydrothermal depolymerization mechanism. It is believed that this effect proceeds via reactions such as solvolysis and acidolysis. The presence of recovered water-soluble organics during the heat-up and conversion is critical to the outcome of Hydrofaction™. They are believed to act as radical scavengers or stabilizers of intermediate products as well as hydrogen donors during heat-up and conversion, thereby inhibiting the formation of undesired char products and promoting the deoxygenation reactions via hydrogenolysis. For example, it is known that phenol can reduce or inhibit coke formation during lignin degradation [14]. The depolymerization of lignin by hydrolysis is promoted by the presence of phenols. An additional beneficial effect appears to be that the presence of water-soluble organics in the feed inhibits further formation of water-soluble organics, thereby increasing the relative amount of oil produced.

2.3 Benefits of oil recirculation

The addition of recycled oil into the feedstock slurry increases the homogeneity of the feed mixture by facilitating partial dissolution of the biomass. This improves the rheological properties of the incoming slurry, making it more pumpable. The significant fraction of organics, especially recycled oil, reduces the energy required for heat-up due to the lower specific heat capacity of organics compared with water. Finally, the recycled oil is believed to act as radical scavenger or stabilizer of intermediate products during heat-up and conversion, similarly to the water-soluble organics in the aqueous phase.

2.4 How do homogenous alkali metal catalysts benefit the process?

Homogeneous catalysts in the form of potassium, and to lesser degree sodium, are well known to catalyze the degradation of macromolecules by hydrolysis, decarboxylation, and depolymerization type of reactions, as well as inhibit formation of tar, char, and coke. At alkaline conditions, potassium in near-critical and supercritical water is further known to promote water gas shift (WGS) and steam reforming reactions as well as gasification [5, 6, 15].

Carbonate is the preferred form of the potassium salt as CO_2 is an important reaction product from the decarboxylation and gasification reactions. The presence of carbonate/bicarbonate is believed to increase hydrogen production due to changes in the gaseous equilibrium and accelerate WGS as well as steam-reforming reactions. Further, the presence of carbonate/bicarbonate appears to accelerate the depolymerization by hydrolysis during pre-treatment and improve the rheological properties of the slurry.

The pH is important for the reactions to proceed as desired, particularly the production of in situ produced hydrogen via WGS reactions. Hence, the pH is controlled so that sufficient buffer capacity is present in the feed to maintain the pH

alkaline throughout the process. At low pH, the H_2/CO ratio may be close to 1, whereas the ratio is typically in the range of 20–100 at alkaline conditions, indicating both that CO is consumed and that more hydrogen is produced. Additionally, significant amounts of char are observed at acid conditions, whereas no or only small amounts are detected at alkaline conditions.

The reasoning behind the characteristics of the Hydrofaction™ process is discussed above, whereas the following will focus on biomass composition and the chemistry during decomposition and conversion.

3 Biomass composition and conversion

Biomass is biological material derived from recently living organisms; in the context of the energy industry, it mostly refers to plant materials such as wood, straw, seeds, and leaves, as well as animal manures and the organic fraction of municipal solid and sewage wastes. Hydrofaction™ can process most types of biomass, although at present time, mostly focuses on lignocellulosic forest biomass, which is readily and commercially accessible in large aggregated volumes and derived from wood harvest and processing residues including tree branches, bark, leaves and limbs, non-merchantable wood, wood pulp wastes, and sawdust [16]. Lignocellulosic biomass is a complex structural material found in the cell walls of woody plants and consists of cellulose and hemicellulose polysaccharides as well the lignin aromatic polymer (Fig. 5). Proteins, resins, and inorganic matter are also present in minor concentrations. The exact proportion of each component varies among plant genotypes and even among phenotypes, as indicated in Table 1.

Cellulose is an unbranched homopolysaccharide consisting of repeat cellobiose (glucose dimer) units, which are connected to each other with β (1 → 4) glycosidic bonds. A large proportion of cellulose is crystalline due to a characteristic configuration in which cellulose chains are aligned in parallel to each other to allow a very tight network of intermolecular and intramolecular hydrogen bonds [17, 18]. This makes crystalline cellulose very resistant to chemical or biological decomposition. However, this crystallinity is not expected to interfere with biomass decomposition at supercritical conditions, as it has been reported that cellulose undergoes crystalline-to-amorphous transformation in water at around 320 °C and 250 bar [19]. Likewise, alkaline aqueous solutions are known to interfere with cellulose crystallinity, thus making cellulose chains more accessible to degradation [20].

Hemicelluloses, as opposed to cellulose, are a collection of fully amorphous, branched heteropolysaccharides with shorter

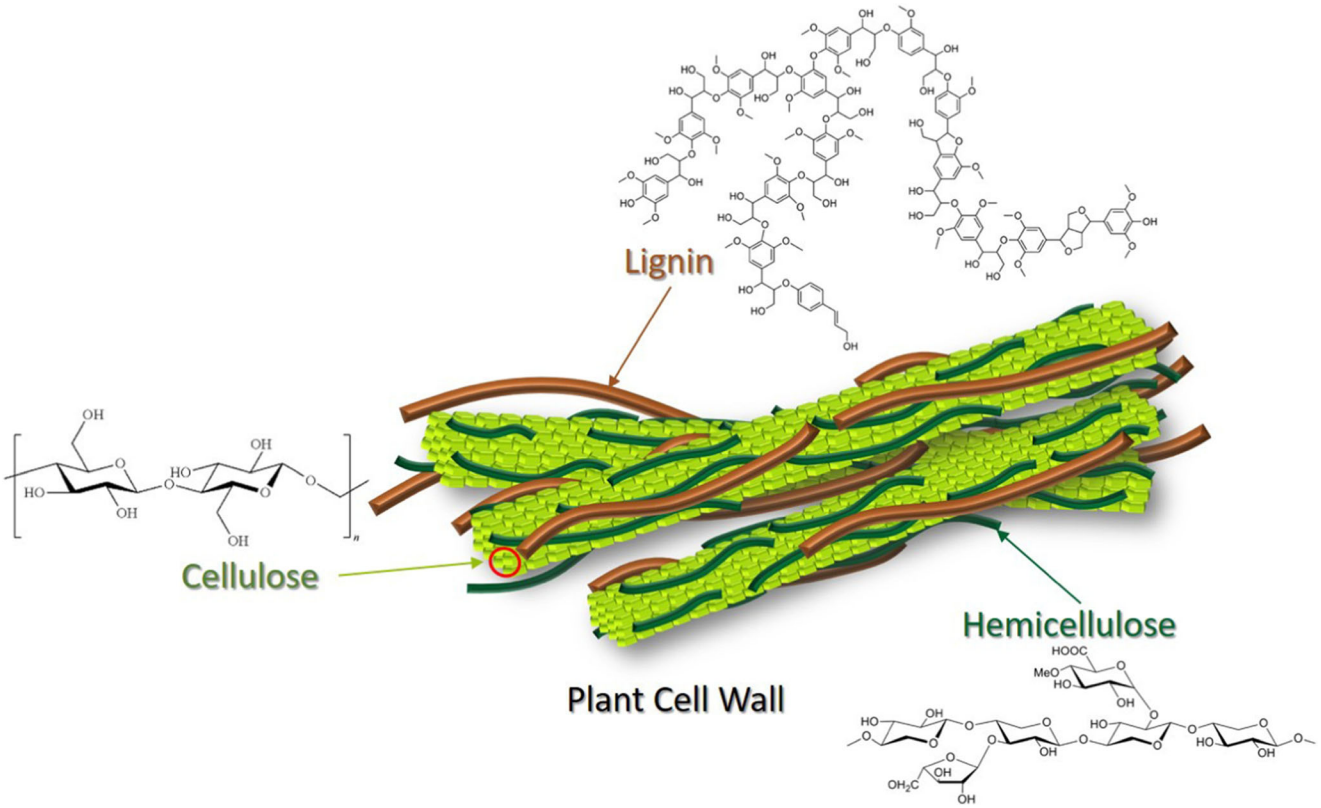

Fig. 5 Structure of lignocellulosic biomass

Table 1 Typical biomass and waste compositions (wt.% dry mass, average) [23]

Lignocellulosic materials	Cellulose	Hemicellulose	Lignin	Ash
Hard woods				
Poplar	46.2	24.4	24.5	1.1
Birch	40.6	29.6	20.2	0.6
Willow	60.5	29.9	25.6	2.2
Eucalyptus	43.2	22.5	25.0	1.6
Soft woods				
Spruce	44.1	21.2	26.9	0.9
Pine	43.6	24.9	25.6	0.7
Coniferous wood	57.5	22.5	30.0	0.4
Douglas fir	45.4	20.9	26.1	1.3
Forest residues				
Bark, pine	23.7	24.9	50.0	3.8
Wood stems	42.6	22.3	37.7	
General residues	45.5	21.0	27.3	
Other lignocellulosics				
Corn stover	38.3	25.2	14.8	6.1
Sugarcane bagasse	37.3	35.8	20.1	5.7
Wheat straw	37.9	26.8	18.3	6.2
Miscanthus	44.6	23.9	21.3	3.7
Switch grass	37.1	31.2	8.5	6.3

chain lengths. They consist of combinations of hexoses (C_6) and pentoses (C_5) as well as uronic acids and acetyl groups, and the combinations vary characteristically between plant species or even plant tissues [21]. Finally, lignin is a complex non-linear macromolecule resulting from the polymerization/cross-linking (via C–C and C–O–C ether bonds) of the following three phenypropanoid units: *p*-coumaryl, coniferyl, and sinapyl alcohols. Similar to hemicellulose, the proportion of these lignin monomers depends on the plant species and tissues [22].

At the plant cell wall structural level, cellulose molecules align in parallel to form the rod-like cellulose microfibrils (Fig. 5). These microfibrils intertwine (to form macrofibrils), leaving some spaces in between which are filled with lignin and hemicelluloses [24]. Lignin and hemicellulose form co-valent bonds (ester and ether) with each other but not with cellulose. Adhesion between cellulose and hemicelluloses is provided by hydrogen and van der Waals forces [22].

From an elemental composition viewpoint, lignocellulosic biomass is mainly comprised of carbon, hydrogen, and oxygen. As an example, Table 2 lists the composition of the sawdust blend that was processed at the pilot plant to produce the oil results discussed in the present article. The oxygen content in lignocellulosic biomass is high, and as mentioned above, this is undesirable for the production of transport biofuels that are functionally indistinguishable to their petroleum counterparts. Oxygen content is also responsible for the low energy density of biomass. More specifically, the 50/50 mix of spruce and pine wood given in Table 2 has the empirical stoichiometric formula $CH_{1,47}O_{0,65}$, whereas liquid hydrocarbon transportation fuels may be represented by the formula $CH_{1,8–2,0}$. Therefore, production of liquid hydrocarbon transportation fuels from lignocellulosics like wood is fundamentally about deoxygenating the biomass, while increasing the H/C ratio.

3.1 Reaction chemistry

The reaction chemistry of hydrothermal liquefaction is complex, and a plethora of chemical reactions may proceed depending of the specific operating conditions. A proposed scheme for the major reactions at Hydrofaction™ conditions is visualized in Fig. 6. The reaction scheme will be used to explain the decomposition and deoxygenation of biomass to renewable oil in an alkaline supercritical water-organic reaction media. It is important to acknowledge that different transition stages, such as heating and cooling, occur along the conversion from biomass to renewable oil. The rate of the individual reactions and the extent to which conversion proceeds via specific reaction pathways differ between these transition stages. Figure 7 provides a conceptual depiction of which major reactions (given in Fig. 6) are favored at the different reaction regimes during the conversion from biomass to renewable oil.

3.2 The heat-up transition stage

During biomass slurry pre-treatment, alkaline conditions and organic solvents facilitate dissolution of the lignocellulosic to its major macromolecules, which are hemicellulose, cellulose, and lignin.

In the initial heat-up transition stage at temperatures up to the critical point, the ionic product of water is high above 10^{-12} and the reaction medium can be considered as completely ionic. The macromolecules depolymerize to oligomers and

Table 2 Elemental composition and higher heating value of spruce and pine on a DAF basis

	Spruce	Pine	50/50 mix	Standard
Carbon (wt.%)	50.4	50.2	50.3	ASTM D 5291
Hydrogen (wt.%)	6.1	6.2	6.2	ASTM D 5291
Oxygen (wt.%)	43.1	43.4	43.3	Balance
Sulfur (wt.%)	0	0	0	ASTM D 1552
Nitrogen (wt.%)	0.2	0.1	0.2	ASTM D 5291
Chloride (wt.%)	0.008	0.007	0.008	ASTM D 808 (mod.)
HHV (MJ/kg)	20.2	20.1	20.2	ASTM D 240

All analyses were performed at the certified laboratory at Uniper, Karlshamn, Sweden

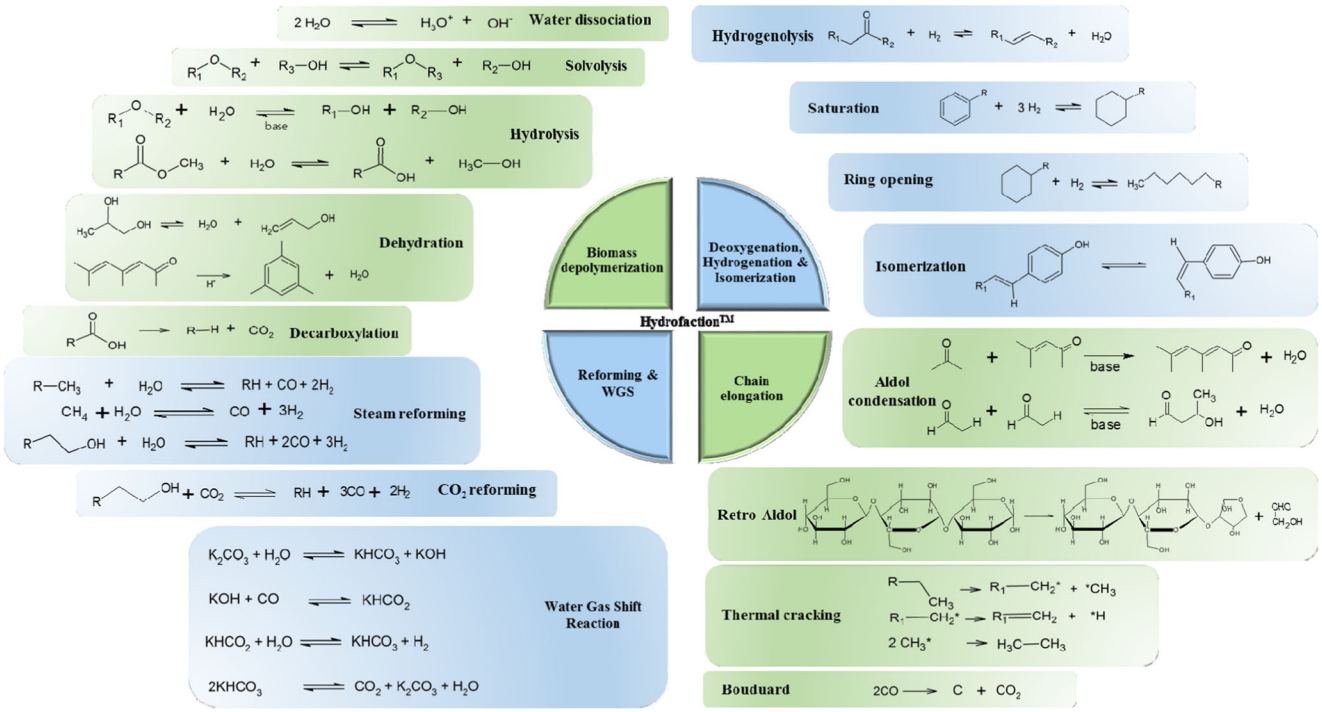

Fig. 6 Major chemical reactions occurring during Hydrofaction™

eventually monomers through alkaline hydrolysis and solvolysis type of reactions. The hydrolysis and solvolysis reactions cleave the glycosidic bonds in hemicellulose and cellulose and the intermolecular ether bonds in lignin.

Hemicellulose depolymerizes first due to its amorphous structure. Cellulose and crystalline cellulose in particular are more resilient to depolymerization, and depolymerization occurs at more severe temperatures. The oligomers and monomers formed from hydrolysis and solvolysis further dehydrate and isomerize to carboxylic acids, aldehydes, and enols, which may further react via decarboxylation and repolymerize via aldol condensation reactions.

The hydrolysis and solvolysis in this region are mainly of heterogeneous nature and therefore associated with a relatively

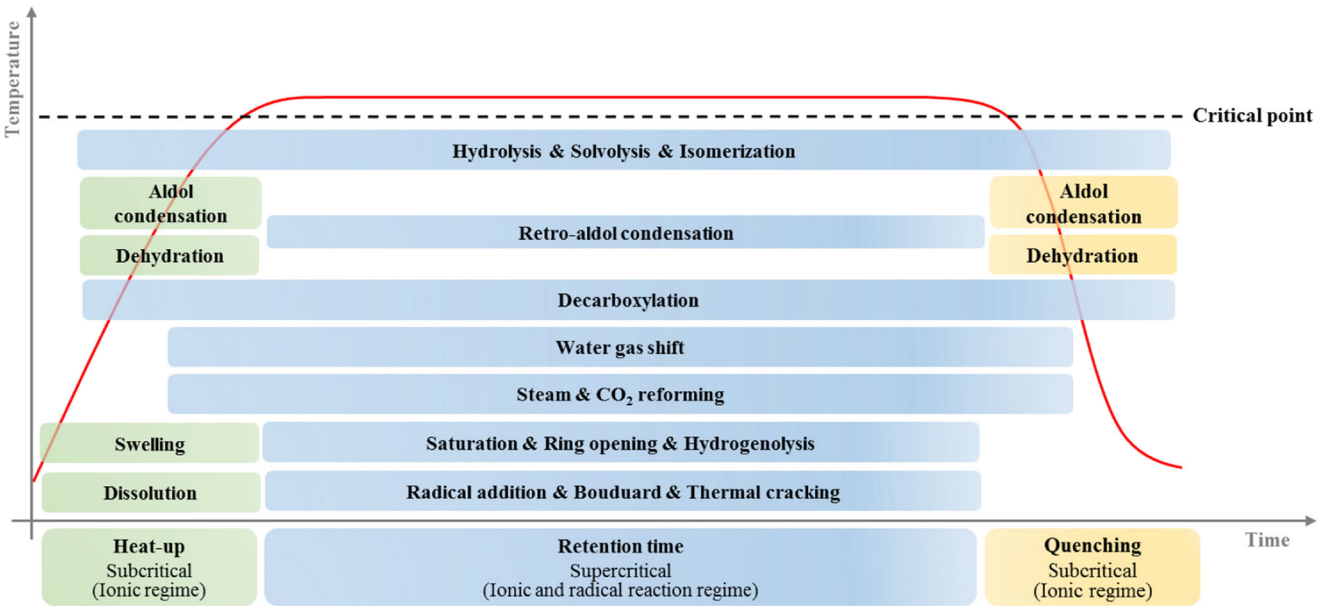

Fig. 7 Visualization of the major reactions occurring in different transition stages of Hydrofaction™

slow dissolution rate in water. Hence, a slow heat-up stage (e.g., <10 °C/min) as for most batch autoclave experiments [5, 6, 8, 9] means that the macromolecules will eventually be depolymerized to monomers. As limited competing reaction options are present in this region, a risk of significant dehydration and condensation reactions similar to caramelization of sugars exists due to the long residence time.

Lignin depolymerization can also take two main pathways, an ionic pathway through the hydrolysis/solvolysis of intermolecular ether bonds leading to the formation of low molecular weight phenolics and a radical pathway through the thermolytical cleavage of both ether and C–C bonds. The high-density water, presence of alkali metal catalysts under alkaline conditions, and perhaps most importantly the recycled organics favor the ionic pathway through hydrolysis/solvolysis of cleaving the ether bond, thereby minimizing the formation of char or high molecular weight compounds through radical addition reactions. Similar findings have been observed by Roberts, Saisu, Okuda, and Pedersen [15, 17, 18, 25].

Hydrofaction™ applies a rapid heat-up (>450 °C/min), whereby the initial heat-up phase is completed within seconds compared to hours for batch reactors [26]. Thereby, undesired reactions such as dehydration and aldol condensation proceeds to a lesser extent until more reaction options are available.

As temperature increases and approaches the critical point of water, rapid dissolution of cellulose occurs and its hydrolysis is greatly accelerated by overcoming mass transfer limitations. This homogeneous type of hydrolysis favors the formation of cellulose oligomers as opposed to monomers [27]. Further alternative reaction options in the form of an alkali metal and base-induced ionic type water gas shift and reforming reactions with water and CO_2 become increasingly important.

Thus, with a rapid heat-up, the effect of the heat-up transition stage is reduced, and the major conversion is occurring at the supercritical reaction regime, in which water gas shift, reforming, and homogenous hydrolysis and solvolysis reactions are favored.

3.3 The supercritical reaction regime

The high-density, alkaline supercritical water applied in Hydrofaction™ promotes further depolymerization of macromolecules through homogeneous hydrolysis and solvolysis rather than pyrolytic cleavage and retro-aldol reactions [15, 27, 28]. Water dissociation catalyzes additional ionic reactions such as isomerization, saturation, and hydrogenolysis. However, due to the relatively severe temperature exploited, radical reactions should also be considered in the supercritical regime. Radical reactions may potentially propagate into coke formation or shift the selectivity towards high molecular weight species, which induces the risk of reactor fouling. With that in mind, Hydrofaction™ utilizes radical scavengers in various forms to participate in chain-terminating reactions. Water acts as a radical scavenger due to its hydrogen-donating ability [11, 12]. Reducing gasses produced in situ such as H_2 and CO are also known to stabilize fragmented radicals and improve biocrude quality during HTL [11, 29, 30]. Additionally, recirculation of organics is believed to improve the impact of free-radical chemistry for two reasons. Firstly, the organics act as radical scavengers with their polar and often reactive carbonyl, carboxyl, and hydroxyl functional groups [30]. Secondly, it is beneficial to increase the concentration of low molecular weight species in relation to radical addition reactions, because they limit the possible chain length of the obtained product [17, 28]. A similar method, though using a heterogenous metal catalyst, is utilized in petrochemical hydroprocessing of heavy residues, where thermal cracking is stabilized by immediate hydrogenation in the presence of hydrogen [31].

The high-density supercritical water appears to provide sufficient solubility of the alkali metal catalysts, and it promotes ionic WGS and reforming reactions, which are considered crucial [11]. To enable the benefits of hydrogen produced in situ, the WGS reactions are promoted by alkaline conditions and in particular by the presence of potassium carbonate. At these conditions, the WGS equilibrium is shifted in the desired direction of a high H_2/CO ratio [32]. This statement is supported by the steady state product gas composition presented later in Table 4, in which the H_2/CO ratio is around 80 and the CO concentration is low at 0.29 wt.%. CO is a prerequisite for WGS reactions, and the CO intermediate is formed by steam and CO_2 reforming that are favored over, e.g., aldol condensation in the supercritical transition stage. Steam reforming facilitates an appealing compromise between gaining hydrogen from the water by sacrificing a carbon and often removing oxygen from the biomass.

Based on the above, reforming reactions followed by WGS are also considered the main pathway for formation of CO_2, which is the most abundant compound in the gaseous product. Decarboxylation is another potential pathway to CO_2 formation, but the effect of decarboxylation is suppressed by the rapid heat-up.

Hydrogen produced from the reforming and water gas shift reactions reacts further through hydrogenolysis of functional groups and hydrogenation type of reactions.

The reactions characteristic to the supercritical operating regime are quenched during subsequent cooling from supercritical conditions to ambient. As indicated in Fig. 7, the reaction products are passing through the purely ionic reaction regime, where dehydration and condensation reactions are favored. Like the initial heat-up transition stage, the cooling is preferably fast to avoid exothermic polymerization and condensation reactions that impose the risk of forming high molecular weight compounds.

The above describes how a complex plethora of reactions need to be carefully controlled to proceed in synergy in the reaction media to liquefy and deoxygenate the biomass into renewable oil.

Fig. 8 Photos from the Pilot at Aalborg University

4 Pilot plant production of Hydrofaction™ oil

The experimental campaign presented in this section resulted in roughly 1 barrel (>150 kg) of steady state oil produced in a continuous pilot facility (the "Pilot") located at the campus of Aalborg University, Denmark. The Pilot has demonstrated the Hydrofaction™ technology since 2013 and is designed to operate at supercritical water conditions up to 450 °C and 350 bar with a capacity of 30-kg/h slurry throughput. The Pilot was commissioned in 1Q2013, and since then, it has completed more than 4000 h of hot operation, including 1200 oil production hours. The plant has constituted a centerpiece for both the experimental work on Hydrofaction™ oil production and academic research activities [33]. Pictures of the Pilot are given in Fig. 8.

4.1 Experimental procedure

A process flow diagram of the Pilot is given in Fig. 9 and described in the following. The pilot is heated up by circulating pressurized deionized water until the system has reached desired temperatures [34]. When the desired process conditions have been established, the feed is switched to biomass slurry. Pressurization of the slurry is done by a high-pressure feed pump and subsequently heated in two serially connected heaters before

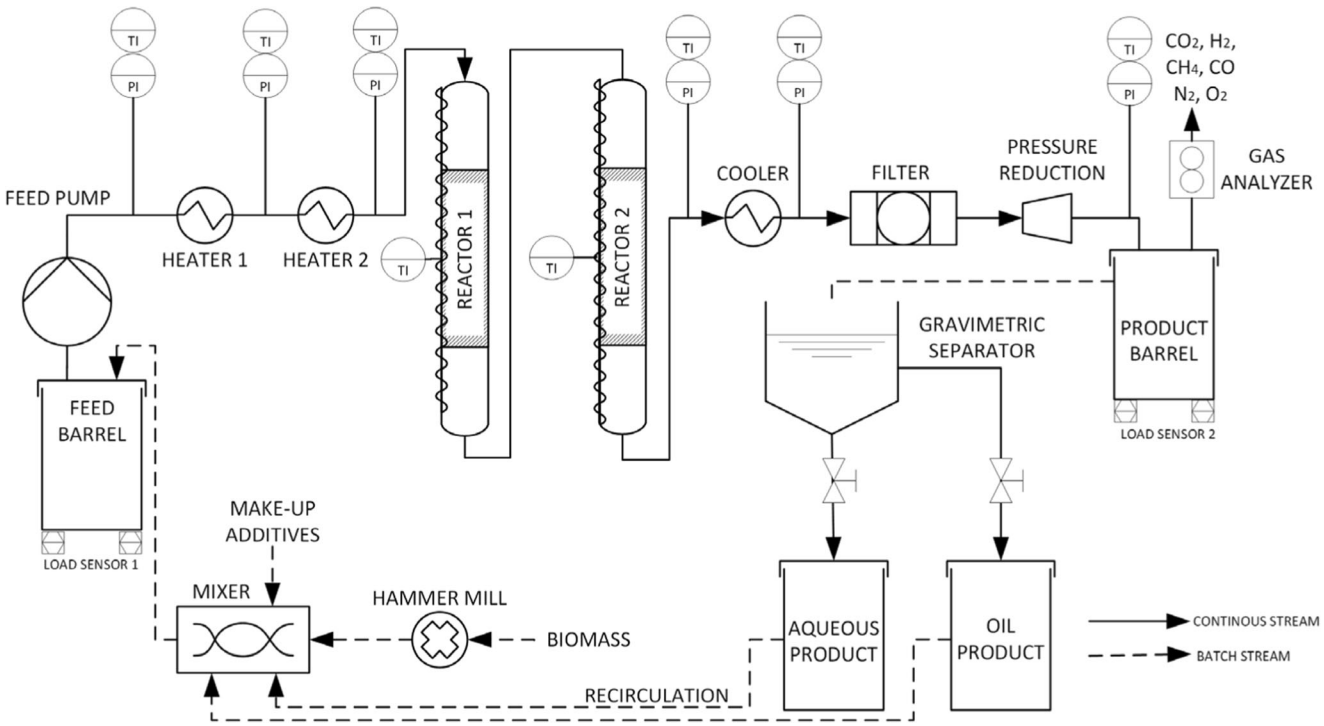

Fig. 9 Process flow diagram of the Pilot

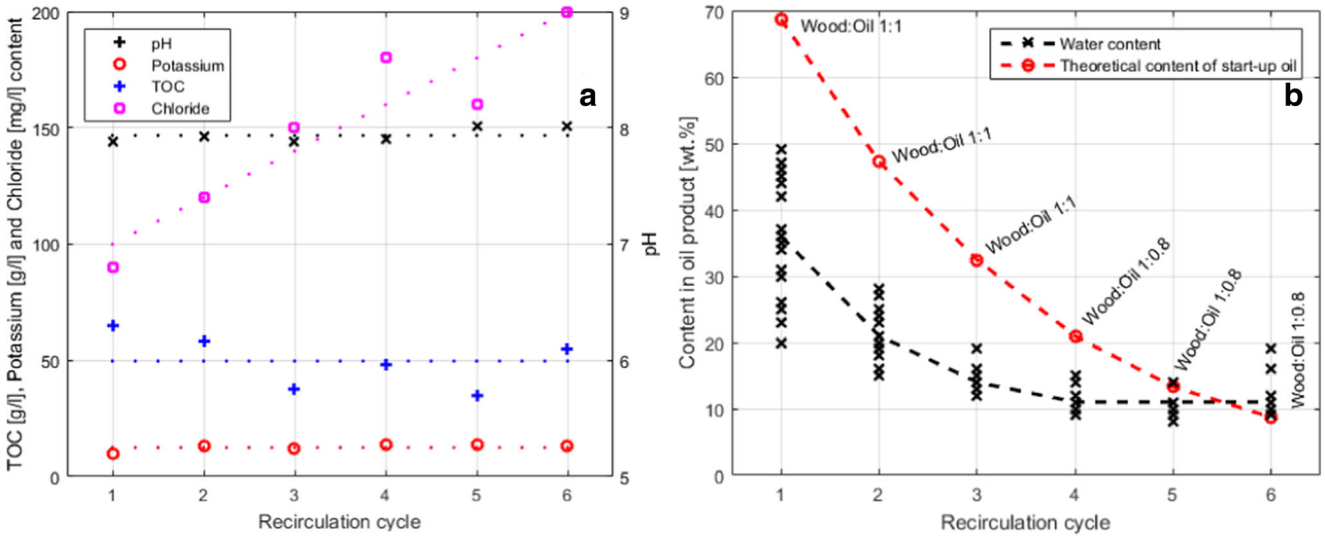

Fig. 10 **a** pH and concentration of potassium, TOC, and chloride in aqueous product as function of recirculation cycle. The analyses are based on Hach-Lange kits for TOC (LCK385), potassium (LCK328), and chloride (LCK311). **b** Water content and theoretical start-up oil content in oil product as function of recirculation cycle. The content of start-up oil is calculated based on the wood to oil ratio in the slurry, the wood to oil yield, and a conservative assumption that the start-up oil does not convert

entering the two 5-L reactors that are kept at 390–420 °C. Reactor effluents are cooled before entering a filtration unit and depressurized in a capillary system [35] prior to degassing the product. The volume flow of gaseous products is measured in an online gas flow meter along with the concentrations of CO_2, H_2, CH_4, CO, N_2, and O_2. Detailed gas compositions are analyzed by SP Technical Research Institute of Sweden by sampling in dedicated gas bags. Liquid products are sampled every 60 min to obtain three to four mass balances per run. An aqueous and an oil product phase are collected and weighed after gravimetric separation in a funnel for 60–90 min at ambient temperature. Prior to recirculation, the aqueous product is analyzed for potassium, ash, total organic carbon (TOC) content, and pH, while the oil product is analyzed for water and ash content. Thereby, the amount of makeup catalyst required in the feed slurry for the consecutive cycle can be determined, and oil can be recirculated on a dry ash-free (DAF) basis.

A homogenous and pumpable slurry is prepared batchwise (100 kg) by mixing wood, milled to a particle size of less than about 2 mm, with recycled aqueous phase, recycled oil, and makeup catalyst. Each slurry batch comprises 17–20 wt.% of wood and 17–20 wt.% of recycled oil on a dry ash-free basis. The balance is made of aqueous effluent from the previous pilot run containing water-soluble organics and alkali metal catalysts. Makeup K_2CO_3 is added as homogeneous catalyst to a slurry concentration of 2.5 wt.% by balancing with the concentration in

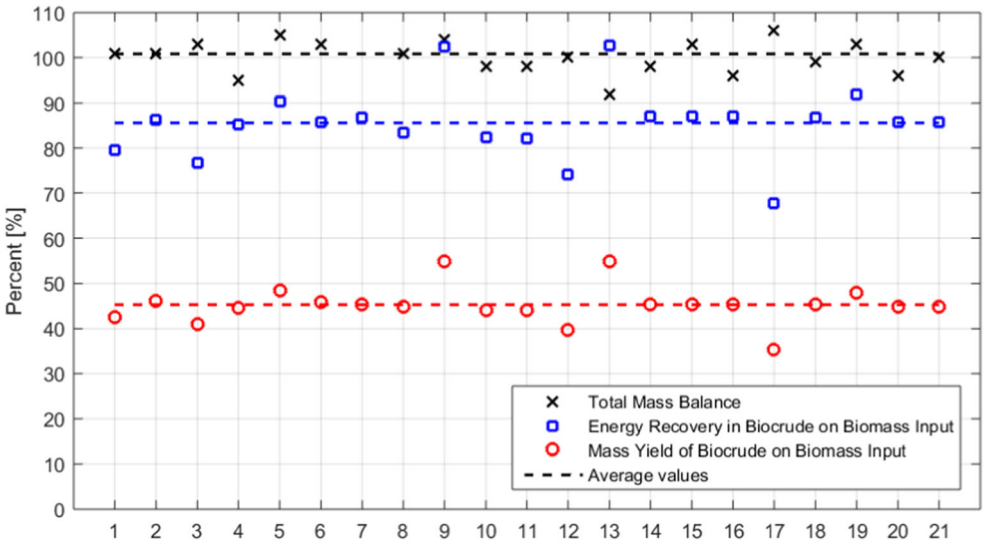

Fig. 11 Key numbers on efficiency for steady state production of biocrude. Total mass balance reflects overall mass balance closure of input and output streams. Energy recovery expresses how much of the energy in the incoming wood is recovered in the biocrude and does not include external utilities. Note that the mass balances presented do not include runs with less than five consecutive recycling of oil and water

the recirculated water product. The pH is adjusted by adding sodium hydroxide to ensure a pH >8.0 in the aqueous product. Stable pH and potassium levels as well as a rather stable TOC content are shown in Fig. 10a as a function of recirculation cycles. At initiation of a new pilot demonstration campaign, the oil and aqueous effluent of the previous run is not available so crude tall oil is used as start-up oil, while 4.5 wt.% ethanol is added to deionized water to emulate water-soluble organics. As such, each run recycles portion of the oil and the water product of the previous run. Figure 10b depicts that the water content of the oil product reaches a steady level after four recirculation cycles. Likewise, the figure shows that the theoretical content of start-up oil in the oil product is <15 wt.% after five recirculation cycles. Based on this, five consecutive cycles have been defined as a minimum to reach steady state, and unless stated otherwise, the results presented are from mass balances collected during fifth- and sixth-cycle runs only.

4.2 Mass, energy, and elemental balances

All mass and energy balances reported in this document are based on data garnered from the steady state operation of the pilot at conditions described above and using the 50/50 wt.% wood mixture listed in Table 2. Figure 11 depicts oil yield, energy recovery, and mass balance closure for a number of mass balances collected during fifth- or sixth-cycle runs. The average values are given in Table 3 together with elemental balances for carbon, oxygen, and hydrogen. Mass yields and elemental composition of raw material and products were used in the determination of elemental balances. The yield of water is based on complete closure of the oxygen balance, assuming that all oxygen from the fed biomass that is not embraced in the oil or forming gaseous species is converted to water. The hydrogen balance is derived from the oxygen balance, and any errors in the previous assumption accumulate in the hydrogen balance. On that basis, an elemental hydrogen balance closure of 114% is considered acceptable.

The overall mass balance is determined to be on average 100.3 wt.%, showing that no mass is accumulated within the plant. The filter, depicted in Fig. 9, is only in place to protect the capillaries from particles, and it did not affect the mass balances. No significant amounts of char or other retentate products were collected in the filter, and any potential char or coke particles must be dispersed in the oil product. This supports the hypothesis that char formation is inhibited by the Hydrofaction™ conditions. The oil yield, defined as the mass of dry ash-free oil produced per mass of dry ash-free biomass fed, is on average 45.3 wt.%. Note that in the presented oil yield, the recycled oil is accounted for and subtracted from the produced oil. The average energy recovery of 85.6% is defined to be energy in the dry ash-free wood that is recovered in dry ash-free produced oil. The gas has a heating value of 7.73 MJ/kg (Table 4), which corresponds to an energy recovery of 15.8%. Extrapolations on a system with heat exchange indicate that if this energy is utilized for energy production (heat), it will release more than enough to make the process self-sustained with heat.

Elemental balances of carbon, oxygen, and hydrogen at steady state conditions are listed in Table 3. The products of the Hydrofaction™ process are oil, gas, and water, of which just oil and gas contain biomass carbon. The aqueous phase that is recycled does contain carbon, but the carbon content is rather constant as function of recirculation cycle as shown in Fig. 10a. This indicates that an even amount of carbon is lost to and gained from the aqueous phase, emphasizing how the aqueous phase

Table 3 Mass, energy, and elemental balance of Hydrofaction™ oil production, based on average values of the runs presented in Fig. 11

		Feed (wood)	Oil	Off gas	Water[a]	Total out
Mass and energy balance						
Mass	wt.%	100	45.3	41.2	13.8	100.3
Energy	%	100	85.6	15.8	0	101.4
Elemental balance						
C	wt.%	100	73.7	26.2	0	99.9
O	wt.%	100	10.5	61.1	28.4	100.0
H	wt.%	100	63.8	25.4	25.1	114.3

Elemental balances reflect the distribution of feedstock elements in the products

[a] Determined based on 100% oxygen balance

Table 4 Steady state gas composition for the product gas

Component	vol.%[a]	wt.%[a]	HHV (MJ/kg)	Standards
H_2	25.79	1.69	2.40	SS-ISO 6974
CO_2	61.14	87.27	0.00	SS-ISO 6974
CO	0.32	0.29	0.03	SS-ISO 6974
CH_4	7.20	3.75	2.08	SS-ISO 6974
Ethene	0.17	0.16	0.08	SS-ISO 6974
Ethane	2.36	2.31	1.20	SS-ISO 6974
Propene	0.29	0.40	0.19	SS-ISO 6974
Propane	1.02	1.46	0.74	SS-ISO 6974
Sum C_4	0.68	1.25	0.62	SS-ISO 6974
Methanol	0.44	0.46	0.10	SS-ISO 6974
Ethanol	0.29	0.43	0.13	SS-ISO 6974
Acetone	0.28	0.53	0.17	SS-ISO 6974
Total	100	100	7.73	

The gas analyses were performed by the certified analysis laboratory at SP Technical Research Institute of Sweden, Sweden. The gas samples were supplied to the laboratory in special designed sample bags dedicated for gas samples. Based on the given composition, the elemental content of the gaseous product is 32 wt.% C, 3.8 wt.% H, 0.0 wt.% N, and 64.1 wt.% O

[a] Air free

Table 5 Hydrofaction™ oil characteristics

Test	Unit	Hydrofaction™ oil	Standard
Elemental analysis (DAF)	wt.%		
C		81.4	ASTM D5291
H		8.7	ASTM D5291
N		0.095	ASTM D5291
S		0.01	ASTM D2622
O		9.8	By difference
H/C mole ratio (DAF)	–	1.28	Calculated
HHV (DAF)	MJ/kg	38.6	ASTM D4809
Water content	wt.%	0.8	ASTM D6304
Density	kg m^{-3}		
At 40 °C		1,057.2	ASTM D4052
At 50 °C		1,050.3	ASTM D4052
At 60 °C		1,043.5	ASTM D4052
At 70 °C		1,036.8	ASTM D4052
Kinematic viscosity at 40 °C	mm^2/s	17,360	ASTM D445
Kinematic viscosity at 60 °C	mm^2/s	1,545	ASTM D445
Total acid number	mg KOH/g	8.8	ASTM D664
Strong acid number	mg KOH/g	<0.01	ASTM D664
Pour point	°C	24	ASTM D97
Flash point	°C	59	ASTM D97

All analyses of the oil were performed by the certified oil laboratory at Saybolt Nederland B.V. Dehydration of the oil by distillation (ASTM D2892) was also done by Saybolt Nederland B.V., and the oil characteristics reflect the dehydrated oil

recirculation improves the mass, energy, and carbon efficiencies by avoiding carbon loss to the aqueous phase. Although, as mentioned in Sect. 2.2, water needs to be purged from the process, because water is added both as biomass moisture and by the water generated during conversion. Thus, in a fully continuous scaled-up system, an aqueous purge stream will be purified to TOC levels low enough to allow disposal, while the majority of the TOC is recycled back into the process through a concentrated aqueous product. Additionally, a purge of the concentrate is required to avoid buildup of wood impurities such as chloride, which is given in Fig. 10a. The loss of TOC through this purge depends on the water treatment technology but is expected to be 1–3 wt.% of the feedstock carbon. This provides some background on the assumption that no or negligible quantities of carbon are lost to the water effluent.

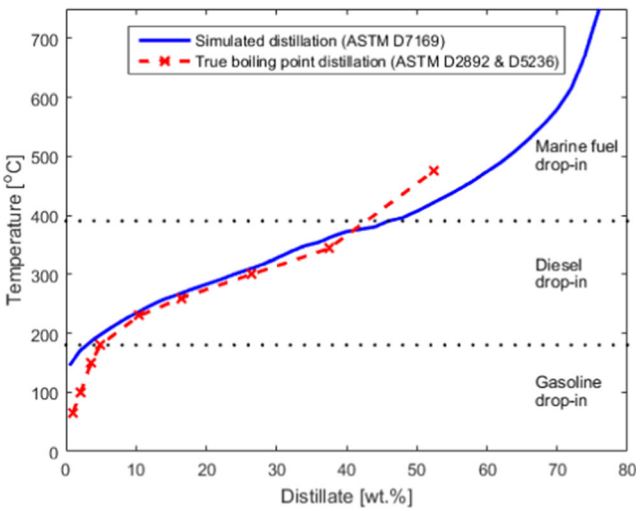

Fig. 12 True and simulated boiling point distribution of dehydrated Hydrofaction™ oil

The oil has a carbon content of 81.9 wt.%, which with the given yield corresponds to a wood to oil carbon recovery of 73.7 wt.%. Likewise, 26.2 wt.% of the feedstock carbon is recovered as gaseous products, resulting in a carbon balance closure of 99.9 wt.%.

The oxygen balance in Table 3 shows that 10.5 wt.% of the biomass elemental oxygen is traced in the oil and 61 wt.% in the gaseous products. This complies with the overall objective of maximizing deoxygenation of the biomass to improve energy density with minimal loss of carbon and hydrogen. The molecular gas composition listed in Table 4 shows that CO_2 is the major gas product. This result indicates that almost two thirds of the oxygen is removed via reforming and WGS reactions and to a lesser extent through decarboxylation, whereas about one third is removed as water. Methane and other light hydrocarbons are products of methanation and cracking reactions. The gas

product composition in Table 4 also shows a significant concentration of H_2 (26 vol.%) and a comparably low CO concentration (0.32 vol.%). This highlights that the presence of potassium carbonate in an alkaline supercritical water medium accelerates the water gas shift reaction towards consuming CO and thus favoring in situ H_2 production.

The significant yield of gaseous products with a higher heating value of 7.73 MJ/kg enables the Hydrofaction™ process to be self-sustained with heat when in steady state. Alternatively, the significant hydrogen production that is characteristic to the technology can be utilized in the downstream oil upgrading, where costly hydrogen is used to upgrade the biocrude to biofuel blendstock. On a biocrude mass basis, 1.5 wt.% H_2 is produced in situ during conversion of wood, which constitutes a significant share (~50%) of the overall H_2 required during upgrading of the Hydrofaction™ oil.

4.3 Hydrofaction™ oil

The oil produced from the continuous steady state pilot plant operations described above has been analyzed by the certified oil laboratory at Saybolt Nederland B.V. for thermophysical properties (Table 5) and distillation properties (Fig. 12). Generally, the oil has properties (oxygen content, H/C ratio, HHV, acid numbers) that make it at least as amenable to upgrading as state-of-the-art, wood-derived HTL oils reported in the literature [5, 6, 8, 9]. It is worth noting that the oil produced from wood is intrinsically low in sulfur (<80 ppm) due to the very low sulfur content in the biomass feedstock. Thus, besides a low carbon footprint, the low sulfur content of Hydrofaction™ oil is a key feature that advances it from petroleum crudes in relation to ultralow sulfur diesel and marine fuel production.

5 Conclusions

The present article covers the characteristics of the Hydrofaction™ technology, from the fundamentals on high-density, supercritical water chemistry with recirculation of organics to operational data from production of 1 barrel of oil in a dedicated pilot plant. The distinctly higher pressures and temperatures applied during Hydrofaction™, relative to the critical point of water and most literature on HTL, maintain a high-water density, thereby enhancing the properties of supercritical water as reaction medium for biomass conversion to renewable oil. Mass, energy, and three elemental balances have been closed for steady state operation, and the reported mass and energy recoveries from wood to oil are 45.3 wt.% and 85.6%, respectively. The oil quality indicates that it is amenable to upgrading to transportation fuel blendstock and can thus contribute to society's imminent challenge of sourcing renewable biofuels that are functionally indistinguishable to existing and carbon-intensive petroleum fuels.

Acknowledgements The authors are thankful for the collaboration with Professor Lasse A. Rosendahl, Aalborg University, Denmark, and the funding provided by EASME Horizon 2020 (Grant No. 666712), Danish Energy Technology Development and Demonstration Program (Grant No. 64013-0513), and Innovation Fund Denmark (Grant No. 4135-00126B).

References

1. US EIA (2016) Short-term energy outlook. Technical report by U.S. Energy Information Administration. https://www.eia.gov/forecasts/steo/report/global_oil.cfm.
2. Ackert S (2013) Aircraft payload-range analysis for financiers. Technical report by Aircraft Monitor.
3. Karatzos S, McMillan JD, Saddler JN (2014) The potential and challenges of drop-in biofuels. Report for IEA Bioenergy Task 39
4. Tews IJ, Zhu Y, Drennan CV, Elliott DC, Snowden-swan LJ, Onarheim K, Solantausta Y, Beckman D (2014) Biomass direct liquefaction options: technoeconomic and life cycle assessment. Technical report 25379 by Pacific Northwest National Laboratory
5. Peterson AA, Vogel F, Lachance RP, Fröling M, Antal MJ Jr, Tester JW (2008) Thermochemical biofuel production in hydrothermal media: a review of sub- and supercritical water technologies. Energy Environ Sci 1:32–65
6. Xue Y, Chen H, Zhao W et al (2016) A review on the operating conditions of producing bio-oil from hydrothermal liquefaction of biomass. Int J Energy Res 40(7):865–877
7. Harvey AH, Peskin AP, Klein SA (2013) NIST/ASME Steam Properties Database, software version 3.0. Standard Reference Database, NIST.
8. Zheng J-L, Zhu M-Q, Wu H-t (2015) Alkaline hydrothermal liquefaction of swine carcasses to bio-oil. Waste Manag 43:230–238
9. Toor SS, Rosendahl LA, Hoffmann J, et al. (2014) Chapter 9, Hydrothermal liquefaction of biomass, 189–217. Book by Springer: Jin F (ed) Application of hydrothermal reactions to biomass conversion, ISBN 9783642544576.
10. Iversen SB (2015) Process and apparatus for producing liquid hydrocarbon. Patent WO2012/167794, issued 21 Apr 2015.
11. Akiya N, Savage PE (2002) Roles of water for chemical reactions in high-temperature water. Chem Rev 102:2725–2750
12. Kruse A, Dinjus E (2007) Hot compressed water as reaction medium and reactant properties and synthesis reactions. J Supercrit Fluid 39:362–380
13. Rutin SB, Skripov PV (2016) Controlled high-power heat release as a tool to selecting working pressure for supercritical water. J Eng Thermophys 25(2):166–173
14. Fang Z, Sato T, Smith RL et al (2008) Reaction chemistry and phase behavior of lignin in high-temperature and supercritical water. Bioresour Technol 99:3424–3430
15. Roberts VM, Knapp RT, Li X, Lercher JA (2010) Selective hydrolysis of diphenyl ether in supercritical water catalyzed by alkaline carbonates. Chem Cat Chem 2:1407–1410
16. Eisentraut A (2010) Sustainable production of second-generation biofuels: potential and perspectives in major economies and developing countries. Technical report by IEA
17. Okuda K, Man X, Umetsu M et al (2004) Efficient conversion of lignin into single chemical species by solvothermal reaction in water–p-cresol solvent. J. Of physics. Condens Matter 16:S1325–S1330
18. Saisu M, Sato T, Watanabe M et al (2003) Conversion of lignin with supercritical water-phenol mixtures. Energy Fuel 17:922–928
19. Deguchi S, Tsujii K, Horikoshi K (2006) Cooking cellulose in hot and compressed water. Chem Commu 31:3293–3295

20. Bali G, Meng X, Deneff JI et al (2015) The effect of alkaline pretreatment methods on cellulose structure and accessibility. Chem Sus Chem 8(2):275–279
21. Klemn D, Philipp B, Heinze T, Heinze U, Wagenknecht W (1998) Comprehensive cellulose chemistry. In: Fundamentals and analytical methods, vol Vol. 1. Wiley-VCH, Weinheim ISBN 9783527294138
22. Sjöström E (1993) Wood chemistry: fundamentals and applications, 2nd edn. Academic press, San Diego ISBN 9780080925899
23. Phyllis2 ECN (2012) Database for biomass and waste. Energy Research Centre of the Netherlands. https://www.ecn.nl/phyllis2/. Accessed 20 Oct 2016
24. Evert RF, Eichhorn SE (2006) Esau's plant anatomy: meristems, cells, and tissues of the plant body: their structure, function, and development, 3rd edn. John Wiley & Sons, Hoboken
25. Pedersen T H, Hydrothermal liquefaction of biomass and model compounds. PhD thesis (2016), Aalborg Universitetsforlag, DK, ISBN 9788771124972
26. Iversen SB (2011) Process and apparatus for producing liquid hydrocarbon. Patent application WO2012/167789, filed 10 Jun 2011
27. Matsumura Y, Sasaki M, Okuda K et al (2006) Supercritical water treatment of biomass for energy and material recovery. Combust Sci Technol 178:509–536
28. Sasaki M, Fang Z, Fukushima Y et al (2000) Dissolution and hydrolysis of cellulose in subcritical and supercritical water. Ind Eng Chem Res 39:2883–2890
29. Davis H, Figueroa C, Schaleger L (1982) Hydrogen or carbon monoxide in the liquefaction of biomass. Paper submitted for the World Hydrogen Energy Conference IV, Pasadena, Ca, US, 13–17 June 1982
30. He BJ, Zhang, Y, Yin Y, Funk TL, Riskowski GL (2001) Effects of alternative process gases on the thermochemical conversion process of swine manure. Trans ASAE 44, 6, 1873–1880
31. Gary JH, Handwerk GE, Kaiser MJ (2007) Petroleum refining: technology and economics, 5th edn. Book by CRC press, ISBN 9780849370380.
32. Kruse A (2011) Behandlung von Biomasse mit überkritischem Wasser. Chem Ing Tech 83(9):1381–1389
33. Pedersen TH et al (2016) Continuous hydrothermal co-liquefaction of aspen wood and glycerol with water phase recirculation. Appl Energy 162:1034–1041
34. Iversen SB (2015) Improved method for preparing shut down of process and equipment for producing liquid hydrocarbons. Patent WO2014/032669, issued 22 Dec 2015.
35. Iversen SB (2014) Pressure reduction device and method. Patent application WO2014/181283, filed 08 May 2014.